

BECs on slightly asymmetric double-well potentials

B. Juliá-Díaz,^{1,2} J. Martorell,¹ and A. Polls^{1,2}

¹*Departament d'Estructura i Constituents de la Matèria,
Universitat de Barcelona, 08028 Barcelona, Spain*

²*Institut de Ciències del Cosmos, Universitat de Barcelona, E-08028 Barcelona, Spain*
(Dated: March 19, 2019)

An analytical insight into the symmetry breaking mechanisms underlying the transition from Josephson to self-trapping regimes in Bose-Einstein condensates is presented. We obtain expressions for the ground state properties of the system of a gas of attractive bosons modeled by a two site Bose-Hubbard hamiltonian with an external bias. Simple formulas are found relating the appearance of fragmentation in the condensate with the large quantum fluctuations of the population imbalance occurring in the transition from the Josephson to the self-trapped regime.

PACS numbers:

I. INTRODUCTION

The dynamics of cold bosonic atoms in double-well potentials has deserved a great deal of attention in the last decade. See [1, 2] for a careful review of the early findings, and [3] for a more recent update. Of particular interest here are the seminal works of Smerzi *et al.* [4] and Milburn *et al.* [5]. The latter managed to derive a simplified many-body hamiltonian with semiclassical predictions similar to those of [4] but with the important advantage of allowing the study of the quantum fluctuations on top of the semiclassical quantum averages. In both cases, the most remarkable feature reported was the existence of a new phenomenon, macroscopic self-trapping, directly linked to the atom-atom interaction. Most of the studies focused on the case of repulsive atom-atom interactions. However, more recently interest has grown on the properties of these systems when this interaction is made attractive and in particular on the appearance of cat like ground states whose description goes beyond the usual semiclassical approximations [6–8]. The structure of these ground states is determined by the ratio between interaction and tunneling strengths.

For repulsive interactions, the Bose-Hubbard model has been widely used to study the transition between the Josephson and the self-trapped regimes [5, 6, 9–11]. It is also the natural choice for attractive interactions. Varying the parameters of the model allows to easily scan the properties of the system. The transition from the Josephson to the self-trapped regime is directly related to the properties of the spectrum of the system as we increase the atom-atom interactions. In a recent manuscript the strongly correlated nature of the ground state of the system (for attractive interactions) in the transition region has been described [12]. This state is similar to the cat-like states described in Ref. [13, 14] for the case of internal Josephson-like behavior. Both studies find a deep relation between the appearance of a bifurcation in the semi-classical description and the existence of strongly correlated, cat-like, ground states in the systems. Similar states also appear in the nucleation of vortices in BECs [15]. The presence of the bifurcation points to the

need of a fully quantum description that goes beyond the usual semiclassical approach. However the exact solution of the Bose-Hubbard model involves numerical calculations that complicate the interpretation of the results. It is thus highly desirable to develop also simplified models that give analytical insights into the relevant physics.

In this article we extend the previous work of Javanainen *et al.* [6], Jääskeläinen and Meystre [7], and the more recent one of Shchesnovich and Trippenbach [8, 16]. Starting from Bose-Hubbard hamiltonians, these authors obtain approximate, Schrödinger-like, equations for the dynamics of the Fock space amplitudes of a system of N atoms on a double-well potential. We will first rederive these equations and, afterwards, will go one step further and obtain simple analytical solutions under certain premises. These are found to be in good agreement with the exact results and help to explain the delicate balances involved in the transition between the two regimes.

II. QUANTUM MODELS FOR THE GROUND STATE

The time dependent Schrödinger equation governing the evolution of the system of N atoms reads,

$$\frac{i}{N}\partial_\tau|\Phi\rangle = \hat{H}|\Phi\rangle, \quad (1)$$

with the (Bose-Hubbard) Hamiltonian written in reduced units as ¹,

$$\hat{H} \equiv -\frac{1}{N}(a_1^\dagger a_2 + a_2^\dagger a_1) + \frac{\varepsilon}{N}\hat{n}_1 + \frac{\gamma}{N^2}(\hat{n}_1^2 + \hat{n}_2^2). \quad (2)$$

Where $\hat{n}_i = a_i^\dagger a_i$, N is the total number of atoms in the system and a_i (a_i^\dagger) is the annihilation (creation) operator for well i . The Fock state basis is written as $|n_1, n_2\rangle$ and

¹ To ease the comparison with the work in [8] we will make use of their notation.

has $N + 1$ vectors, $\{|0, N\rangle, \dots, |N, 0\rangle\}$. The two parameters governing the dynamics are γ , which measures the ratio between the contact atom-atom interactions and the hopping strength, and ε which is a symmetry breaking bias, also divided by the hopping strength². For this study we take $\varepsilon < 0$ which promotes $|1\rangle$.

With this sign convention, $\gamma > 0$ and $\gamma < 0$ correspond to repulsive and attractive atom-atom contact interactions.

The solution to (2) can be expanded in the Fock basis as, $|\Phi(t)\rangle = \sum_{k=0}^N c_k(t) |k, N-k\rangle$, leading to an equation for the time evolution of the coefficients c_k of the form [8]:

$$\frac{i}{N} \frac{d}{d\tau} c_k = -(b_{k-1} c_{k-1} + b_k c_{k+1}) + a_k c_k, \quad (3)$$

with $b_k = \frac{1}{N} \sqrt{(k+1)(N-k)}$, and $a_k = \frac{\gamma}{N^2} [k^2 + (N-k)^2] + \frac{\varepsilon}{N} k$. Now, it is useful to introduce a new variable, $x = k/N$, and, assuming that $h \equiv 1/N$ is small, we define $\Psi(x) = c_k/\sqrt{N}$ and $b(x) = b_k$. The next step is to make x a continuous variable³. This leads to Eq. (5) of [8],

$$ih\partial_\tau \Psi(x) = -[e^{-i\hat{p}} b_h(x) + b_h(x) e^{i\hat{p}}] \Psi(x) + a(x) \Psi(x), \quad (4)$$

where $\hat{p} \equiv -ih\partial_x$, and

$$\begin{aligned} b_h(x) &= [(x+h)(1-x)]^{1/2}, \\ a(x) &= \gamma[x^2 + (1-x)^2] + \varepsilon x. \end{aligned} \quad (5)$$

Eq. (4) describes the time evolution of $\Psi(x)$, which is a continuous interpolation of the c_k/\sqrt{N} . This interpolation assumes a certain degree of smoothness for the c_k , so that for most k : $\text{sign}(c_{k+1}) = \text{sign}(c_k)$. This is the case for the ground state with either repulsive or attractive interactions, provided the symmetric state is lower in energy than the antisymmetric one (our case)⁴.

From the formally exact Eq. (4), we first retain up to terms of order h^2 ,

$$e^{\pm i\hat{p}} \simeq 1 \pm h\partial_x - \frac{1}{2} h^2 \partial_x^2 \quad (6)$$

and

$$b_h(x) \simeq b_0(x) + h\partial_h b_h(x)|_{h=0} + (1/2)h^2 \partial_h^2 b_h(x)|_{h=0}, \quad (7)$$

² To compare to our previous work [12], let's note that, $\Lambda = -2\gamma$, and $\varepsilon_{\text{Ref12}}/J = \varepsilon/2$.

³ Formally, we then have, $b_{k-1} = e^{-h\partial_x} b(x)$, $c_{k-1} = \sqrt{N} e^{-h\partial_x} \Psi(x)$, and $c_{k+1} = \sqrt{N} e^{h\partial_x} \Psi(x)$.

⁴ There are however other cases for which the c_k alternate in sign: $c_k c_{k+1} < 0, \forall k$. One example is the mean field state $\Phi = [(1/\sqrt{2})(a_1^\dagger - a_2^\dagger)]^N |\text{vac}\rangle$ As in [8], one way of dealing with this case is by introducing an auxiliary smooth function $\tilde{\Psi}(x) = e^{i\pi k} \Psi(x)$.

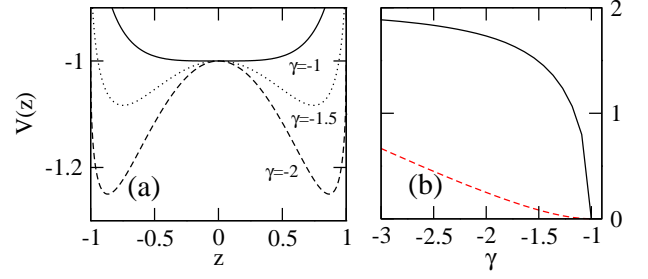


FIG. 1: (color online) (a) The potential \mathcal{V} for several values of γ and zero bias ($\varepsilon = 0$), (b) Separation between the two minima (solid-black) and height of the barrier as function of γ , (dashed-red), also in the case of zero bias.

to get,

$$\begin{aligned} ih\partial_\tau \psi(x) &\simeq -h^2 b_0(x) \psi''(x) - h^2 b_0'(x) \psi'(x) \\ &+ [a(x) + V_2(x)] \psi(x) \end{aligned} \quad (8)$$

where

$$\begin{aligned} V_2(x) &= -2b_0(x) + h(b_0'(x) - 2\partial_h b_h(x)|_{h=0}) \\ &- h^2(\partial_h^2 b_h(x)|_{h=0} - \partial_h b_h'(x)|_{h=0} + \frac{1}{2} b_0''(x)). \end{aligned} \quad (9)$$

This equation is similar to Eq. (13) of [8] if we retain only the h^0 term in $V_2(x)$. This approximation respects the symmetry and behaves well at the edges of the Fock space. Besides, taking into account that,

$$\hat{p} \sqrt{x(1-x)} \hat{p} \psi = -h^2 \partial_x (b_0 \partial_x \psi) = -h^2 (b_0' \psi' + b_0 \psi''), \quad (10)$$

we arrive to

$$ih\partial_\tau \psi = +[\hat{p} \sqrt{x(1-x)} \hat{p} + a(x) + V_0(x)] \psi(x), \quad (11)$$

with $V_0(x) = -2\sqrt{x(1-x)}$.

The range of x is the interval $[0, 1]$. It will be convenient to introduce the variable $z \equiv 1 - 2x$, $z \in [-1, 1]$. In terms of the new variable, Eq. (11) becomes

$$ih\partial_\tau \psi(z) = \left(-2h^2 \partial_z \sqrt{1-z^2} \partial_z + \mathcal{V}(z) \right) \psi(z) \quad (12)$$

with $\mathcal{V}(z) = (1/2)(\gamma z^2 - \varepsilon z) - \sqrt{1-z^2}$. This equation is a Schödinger-like equation with an effective z dependent mass: $-h^2/(2m) \equiv -2h^2 \sqrt{1-z^2}$. For convenience, we normalize $\psi(z)$ as $1 = \int_{-1}^1 dz |\psi(z)|^2$.

As discussed in Refs. [16] and [12], the population imbalance is an appropriate order parameter. It is defined as,

$$I = (\langle \Phi | \hat{n}_2 - \hat{n}_1 | \Phi \rangle) / N = \sum_{k=0}^N c_k^2 (1 - 2k/N), \quad (13)$$

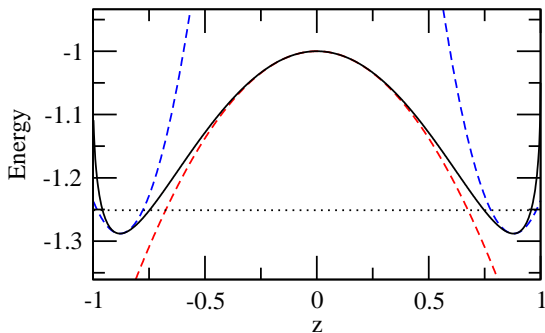


FIG. 2: (color online) The potential \mathcal{V} , black, compared to the three parabola used to approximate it near its extrema in building the analytical model. $N = 50$, $\gamma = -2.1$.

which in the continuous variable reads, $I = \int_{-1}^1 dz |\psi(z)|^2 z$, where we have used $\sum_{k=0}^N c_k^2 = 1$ and the normalization of the $\psi(z)$.

A. Effective two mode model

We first study the solutions of Eq. (12) for the stationary case with zero bias, and concentrate on the region where the classical bifurcation appears, $\gamma < -1$.

For $\gamma < -1$, $\mathcal{V}(z)$ has two symmetric minima, which get deeper as γ decreases, see panel (a) of Fig. 1. The separation between the two minima, $2\sqrt{1 - 1/\gamma^2}$ and the barrier height ($\Delta = (1 + \gamma)^2 / (2|\gamma|)$) are depicted in panel (b).

Since $\mathcal{V}(z)$ has pronounced minima and maximum we first determine the g.s. energy of the system by approximating these minima by parabolas, see Fig. 2,

$$\mathcal{V}(z) \simeq \mathcal{V}(z_m) + \frac{1}{2} \mathcal{V}''(z_m) (z \pm z_m)^2 \quad (14)$$

with $z_m = \sqrt{1 - 1/\gamma^2}$, $\mathcal{V}(z_m) = \gamma/2 + 1/(2\gamma)$, and $\mathcal{V}''(z_m) = \gamma - \gamma^3$. As an additional approximation, in the first term in the r.h.s. of Eq. (12) we replace z by z_m , since the wavefunction, $\psi(z)$, is sharply peaked around the minima at $\pm z_m$. The stationary pseudo-Schrödinger equation can then be written as,

$$\begin{aligned} & \left[-2\hbar^2 \partial_z^2 + \frac{1}{2} (\gamma^4 - \gamma^2) (z - z_m)^2 \right] \psi \\ & = [-\gamma E + (1 + 1/\gamma^2) / 2] \psi \end{aligned} \quad (15)$$

and its spectrum can be readily obtained by comparing to the harmonic oscillator: $\hbar^2/(2m) \rightarrow 2\hbar^2$, $m\omega^2 \rightarrow \gamma^2(\gamma^2 - 1)$ and $\hbar\omega/2 \rightarrow -h\gamma\sqrt{\gamma^2 - 1}$. From this analogy one easily gets the ground state energy:

$$E_{\text{g.s.}} = \frac{1}{2\gamma} + \frac{\gamma}{2} + h\sqrt{\gamma^2 - 1}. \quad (16)$$

This approximation turns out to be very reasonable as it can be seen in Fig. 3 by comparing the g.s. energies

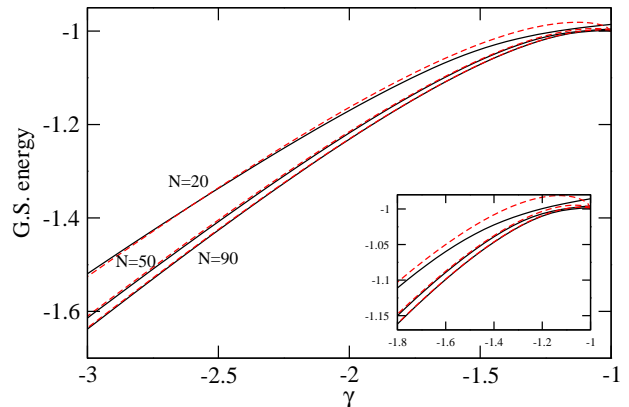


FIG. 3: (color online) Ground state energies of Eq. (12), solid-black, compared to the approximate ones given by Eq. (16), dashed-red, for $N = 20, 50$ and 90 , respectively.

obtained using Eq. (16) and the ones obtained by solving numerically the pseudo-Schrödinger Eq. (12). The approximation is particularly good for large N (small $\hbar = 1/N$), and γ not too close to the bifurcation point, $\gamma = -1$, as shown in the inset of the figure.

For our analysis we assume that the harmonic oscillator estimate of the ground state is accurate enough and that the shape of $\psi(z)$ around z_m (and also $-z_m$) is that of the g.s. harmonic oscillator, i.e. gaussian with the parameters also determined from Eq. (16). These normalized solutions will be denoted $|\mathcal{R}\rangle$ or $\Psi_{\mathcal{R}}^{(h.o.)}(z)$, and $|\mathcal{L}\rangle$ or $\Psi_{\mathcal{L}}^{(h.o.)}(z)$. They correspond to the clockwise and counter-clockwise rotor solutions to the pendulum in the language of Ref. [4]. They form the “two-mode” basis for the model to be described below. Notice also that these two modes are built in the Fock space, they are useful to describe the system during the bifurcation and in the self-trapping regime. In fact, the model works soon after the bifurcation starts, once the overlap $\langle \mathcal{L} | \mathcal{R} \rangle$ is small enough. This overlap is given by, $\exp[2(\gamma^2 - 1)^{3/2} / (\gamma h)]$. As it can be seen in panel (A) of Fig. 4, this overlap (black dot-dashed line) is essentially zero for $\gamma \lesssim -1.05$ and $N = 50$. For these basis vectors, $\langle \mathcal{L} | z | \mathcal{L} \rangle = -z_m$ and $\langle \mathcal{R} | z | \mathcal{R} \rangle = z_m$. In this two-mode model, an approximate solution can be written as:

$$|\psi\rangle = \cos \alpha |\mathcal{L}\rangle + \sin \alpha |\mathcal{R}\rangle. \quad (17)$$

In the absence of bias the ground state is the symmetric combination, and therefore $\alpha = \pi/4$. The expectation value of z in the state (17) is easily calculated, $\langle z \rangle = -z_m (\cos^2 \alpha - \sin^2 \alpha) = -z_m \cos(2\alpha)$. The dispersion of z , $\sigma_z^2 \equiv \langle \psi | z^2 | \psi \rangle - \langle \psi | z | \psi \rangle^2$, can also be readily computed. Retaining up to order \hbar ,

$$\sigma_z^2 = z_m^2 \sin^2 2\alpha - \hbar / (\gamma \sqrt{\gamma^2 - 1}). \quad (18)$$

When no bias is present, $\langle z \rangle = 0$ and $\sigma_z^2 = z_m^2 - \hbar / (\gamma \sqrt{\gamma^2 - 1})$. The large values of σ_z^2 are due to the fact

that the ground state is cat-like, i.e. the wavefunction has two peaks in z .

When a finite but small bias, $|\varepsilon| \ll 1$, is considered, α is determined by the balance between the tunneling across the middle barrier of \mathcal{V} and the bias term. In the absence of tunneling, $|\psi\rangle$ will consist only of $|\mathcal{L}\rangle$ or of $|\mathcal{R}\rangle$ depending on the sign of the bias constant, ε . In the latter situation the main contributor to σ_z is the otherwise small $-h/(\gamma\sqrt{\gamma^2-1})$ term, as the $\sin^2 2\alpha$ becomes negligible.

To take into account both effects, the tunneling across the Fock space barrier and the bias term, we write an effective Hamiltonian for this two-mode model

$$\mathcal{H} = \begin{pmatrix} \varepsilon z_m/2 & -t \\ -t & -\varepsilon z_m/2 \end{pmatrix}. \quad (19)$$

The eigenvalues of \mathcal{H} are $E_S = -\sqrt{t^2 + \varepsilon^2 z_m^2/4} = -E_A$. Thus, one way to obtain the value of the tunneling constant, $t > 0$, is by computing the energy splitting between the symmetric and anti-symmetric states in the double well in the absence of bias, $t = (1/2)\Delta E_{AS} \equiv (1/2)(E_A - E_S)$.

To estimate this energy splitting in the double-well we will neglect the z dependence of the effective mass. This brings our problem to a Schrödinger-like equation and we can make use of the WKB approximation as developed in Razavy's book, [17]. The energy splitting is written in Eq. (3.109) of that book:

$$\Delta E_{AS} = \frac{\hbar\omega}{\pi} \exp\left(-\int_{z_-}^{z_+} \sqrt{(2m/\hbar^2)(\mathcal{V}(z) - E)} dz\right). \quad (20)$$

In our case we use the equivalences given above Eq. (16) to assign values to $\hbar^2/(2m)$ and $\hbar\omega$. The value of E corresponds to the ground-state energy and is taken from the harmonic oscillator approximation defined in Eq. (16). To compute the tunneling integral, and obtain analytic results, we will approximate $\mathcal{V}(z)$ by an inverted parabola, $\mathcal{V}(z) \simeq -1 + \frac{1}{2}(\gamma+1)z^2$, see Fig. 2. This gives an energy splitting,

$$\Delta E_{AS} = -2\frac{h\gamma}{\pi}\sqrt{\gamma^2-1} \exp\left(-\frac{\pi}{2h}\frac{|E|-1}{\sqrt{|\gamma|-1}}\right) \quad (21)$$

This estimate of the splitting in absence of bias, is used to extract the value of t and it is in very good quantitative agreement with the exact energy splitting obtained by solving Eq. (12) in absence of bias or as it will be discussed later, when the bias is not dominant. It is an important improvement on the estimate given in Ref. [8] (cf. Eq. (31)). The value of $2t$ is plotted (red dot-dashed line) in panel (C) of Fig. 4.

From the two mode Hamiltonian (Eq. (19)) we find that the predicted ‘‘full’’ (including the bias) symmetric-antisymmetric energy splitting is

$$\Delta E_{AS}^{(tm)} = 2\sqrt{(\varepsilon z_m/2)^2 + t^2} \quad (22)$$

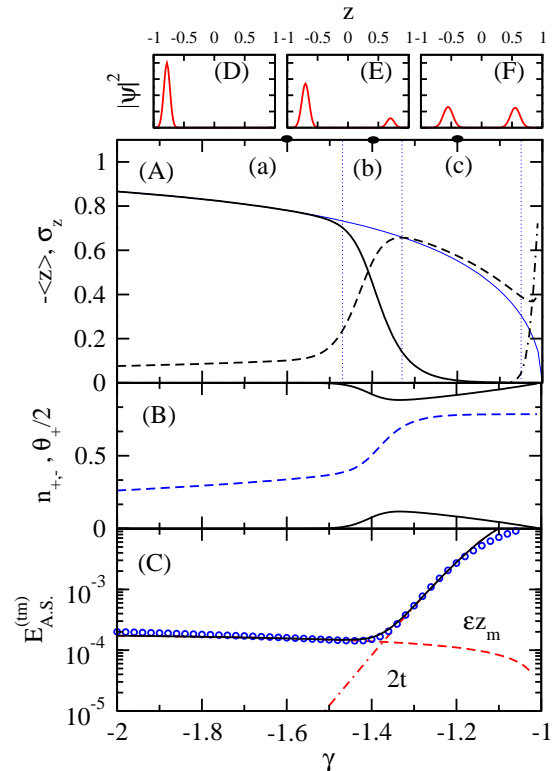


FIG. 4: (color online) The three smaller plots above, (D), (E), and (F), show $|\psi(z)|^2$ computed with the two mode model for $\gamma = -1.2, -1.4$, and -1.6 respectively. (A) Different ground state properties predicted by the analytic model for three different regimes, separated by blue dotted lines. The three regions correspond to the bias-dominated fully-condensed (a), transition-asymmetric cat-like (b), and symmetric cat-like (c). We depict the behavior of $-\langle z \rangle_{g.s.}$, black solid line, and σ_z , black dashed line, as a function of γ . z_m is shown in thin-blue. The overlap $\langle \mathcal{L} | \mathcal{R} \rangle$ is the black dot-dashed line. The middle panel, (B), contains the condensed fractions, n_{\pm} (upper and lower black solid lines), and the mixing angle $\theta/2$ of the φ_+ eigenvector, see Eq. (26), of the one-body density matrix associated to the ground state of the two-mode model. The lower panel, (C), depicts the energy splitting between the symmetric and antisymmetric (ground and first excited) states. The solid black line is calculated with Eq. (22). The blue empty circles are the exact numerical result obtained by solving Eq. (12). Red dot-dashed and red dashed lines depict $2t$ and εz_m respectively. In all cases $\varepsilon = -0.0002$ and $N = 50$.

with two well-defined limits, $2t$ and εz_m (red dot-dashed and red dashed lines of panel (c) of Fig. 4 respectively), depending on whether tunneling or bias is the dominant contribution. The ground state can be readily computed, $\mathcal{H}\psi_S = E_S\psi_S$, with $\psi_S = (\cos \alpha, \sin \alpha)$ and $\tan \alpha = \xi + \sqrt{\xi^2 + 1}$, where, $\xi \equiv (\varepsilon z_m/2t)$.

The one body density matrix for the Bose-Hubbard Hamiltonian can be written as,

$$\hat{\rho} = \frac{1}{N} \begin{pmatrix} a_1^\dagger a_1 & a_1^\dagger a_2 \\ a_2^\dagger a_1 & a_2^\dagger a_2 \end{pmatrix}, \quad (23)$$

with $\text{Tr}\hat{\rho} = 1$. In the large- N model we have, $a_1^\dagger a_1 = (1 + \hat{z})/2$, $a_2^\dagger a_2 = (1 - \hat{z})/2$, $a_1^\dagger a_2 = a_2^\dagger a_1 = \sqrt{1 - \hat{z}^2}/2$. In the two mode model retaining up to order \hbar^1 we get,

$$\hat{\rho} = \frac{1}{2} \begin{pmatrix} 1 + z_m \cos 2\alpha & \sqrt{1 - z_m^2} \\ \sqrt{1 - z_m^2} & 1 - z_m \cos 2\alpha \end{pmatrix} \quad (24)$$

with eigenvalues,

$$\begin{aligned} n_{\pm} &= \frac{1}{2} \left(1 \pm \sqrt{1 - z_m^2 \sin^2(2\alpha)} \right) \\ &= \frac{1}{2} \left(1 \pm \sqrt{1 - \sigma_z^2} \right) + \mathcal{O}(\hbar). \end{aligned} \quad (25)$$

The last equality directly relates the appearance of fragmentation and the quantum fluctuations of the population imbalance measured by σ_z , and holds also in the transition region. Denoting the corresponding eigenvectors by: $\varphi_{\pm} = (\cos \theta_{\pm}/2, \sin \theta_{\pm}/2)$ one finds

$$\tan \frac{\theta_{\pm}}{2} = - \frac{\left[z_m \cos 2\alpha \mp \sqrt{1 - z_m^2 \sin^2(2\alpha)} \right]}{\sqrt{1 - z_m^2}}. \quad (26)$$

B. Results

The quantitative predictions of the analytical model are presented in Fig. 4. The model provides a simple and yet deep understanding of the problem. For $\gamma < -1.5$, region (a), the ground state of the system is completely asymmetric (see the left upper smaller plot of Fig. 4), with a large population imbalance, i.e. it is localized on the well promoted by the bias ($|\mathcal{L}\rangle$ for $\varepsilon < 0$). The location of the wells in the Fock space is measured by z_m . The blue thin line in panel (A) shows z_m , which is a decreasing function of γ and reaches zero at the bifurcation point, $\gamma = 0$. In this regime, the bias dominates completely the hamiltonian of Eq. (19), which therefore is essentially diagonal with eigenvectors $|\mathcal{L}\rangle$ and $|\mathcal{R}\rangle$. In these cases, σ_z is small and given by the spread of the occupied mode. In this region, the system is fully condensate. Correspondingly, as it is shown in the panel (B), the eigenvalues of the one-body density matrix of the ground state, are 1 and 0. In the panel (C), it is clearly shown that $2t$ is very small compared with εz_m , and the splitting $E_{A.S.}^{(tm)}$ (Eq. 22) in this region is given by εz_m .

In region (b) both the bias term εz_m and the tunneling matrix element, t , are of comparable size (see panel (C)). In that region the ground state is an asymmetric cat-like state (see the central upper smaller plot). The value of $-\langle z \rangle$ is decreasing and has large fluctuations, shown in the region (b) of panel (A), mostly due to having both modes populated simultaneously. The system is fragmented into two condensates, i.e the eigenvalues of the one-body density matrix are both different than zero, being φ_+ more populated, see panel (B) of the figure.

The macro-occupied state, φ_+ , varies from close to $|1\rangle$ to $(1/\sqrt{2})(|1\rangle + |2\rangle)$ as can be seen from the behavior of the mixing angle $\theta_+/2$ (blue dashed line in panel B).

The tunneling term, t , grows exponentially and is responsible for the abrupt decrease of z as one crosses into the region, (c). There, the two mode Hamiltonian is dominated by the tunneling matrix element, and the wave function becomes symmetric-cat-like, as shown in the right upper smaller plot. The cat like nature of the state reflects in a small value of the imbalance and a sizeable σ_z . Notice that when γ approaches -1, the two-mode approximation is not valid anymore, because the $\langle \mathcal{L} | \mathcal{R} \rangle$, shown by the black-dot-dashed line in panel (A) is not longer close to zero.

The simplifications of the two mode model capture to a very large extent the features of the initial large- N model, Eq. (12), as can be seen from the comparison of the exact splitting (blue empty circles) between the ground and first excited state and the two-mode one (black solid line), shown in the last panel of the figure.

III. CONCLUSIONS

For attractive interactions, we have discussed here the appearance and properties of the cat states in the transition from the tunneling to the interaction dominated regimes. The semiclassical approach shows that at some critical value of the ratio of atom-atom to tunneling energies, γ , a bifurcation appears. We have constructed an effective “two mode model” built from the solutions corresponding to the branches of the bifurcation. And have shown that it is quite successful in describing not only the average imbalances in the presence of bias but also the quantum fluctuations. The model includes the main quantal effects since its predictions are in good agreement with exact solutions of the Bose Hubbard hamiltonian.

Our starting point is an already developed large- N model [6, 8] which gives accurate numerical predictions for $N \gtrsim 30$. We have managed to obtain analytic expressions valid on the transition region from self-trapped (bias-dominated) to the symmetric cat-like region (dominated by the tunneling term). The main feature is the sharp change of the population imbalance as γ is decreased. It is due to the delicate interplay between the bias and an effective tunneling term with a sharp dependence on γ .

The fact that Eq. (12) captures most of the non-linear dynamics of the original Bose-Hubbard hamiltonian implies that the complex dynamics of systems governed by non-linear terms can be studied very conveniently with pseudo-Schrodinger equations governing the dynamics in Fock space. In these equations the main effects of non-linearity appear through a barrier-like potential. In this way, some of the dramatic consequences of the nonlinearities are mapped into exponentially varying magnitudes in linear systems. We have exploited this advantage to introduce further approximations and construct

a very simple effective two-mode model to reproduce and explain the main properties of the transition.

The authors thank M. Lewenstein for a careful reading of the manuscript. B.J-D. is supported by a CPAN

CSD 2007-0042 contract. This work is also supported by Grants No. FIS2008-01661, and No. 2009SGR1289 from Generalitat de Catalunya.

-
- [1] A. J. Leggett, Rev. Mod. Phys. **73**, 307 (2001).
 [2] L. Pitaevskii, and S. Stringari, *Bose-Einstein Condensation*. (Oxford University Press, Oxford, 2003).
 [3] R. Gati and M.K. Oberthaler, J. Phys. B.: At. Mol. Opt. Phys. **40**, R61-R89 (2007).
 [4] A. Smerzi, S. Fantoni, S. Giovanazzi, and S. R. Shenoy, Phys. Rev. Lett. **79**, 4950 (1997).
 [5] G.J. Milburn, J. Corney, E.M. Wright and D.F. Walls, Phys. Rev. A **55**, 4318 (1997).
 [6] J. Javanainen, M. Yu. Ivanov, Phys. Rev. A **60**, 2351 (1999).
 [7] M. Jääskeläinen, and P. Meystre, Phys. Rev. A **71**, 043603 (2005); Phys. Rev. A **73**, 013602 (2006).
 [8] V.S. Shchesnovich and M. Trippenbach, Phys. Rev. A **78** 023611, (2008).
 [9] J. Ruostekoski and D.F. Walls, Phys. Rev. A **58**, R50 (1998).
 [10] Gh-S Paraoanu, S. Kohler, F. Sols and A.J. Legget, At. Mol. Opt. Phys. **34**, 4689, (2001).
 [11] K.W. Mahmud, H. Perry and W.P. Reinhardt, Phys. Rev. **A71**, 023615, (2005).
 [12] B. Julia-Diaz, D. Dagnino, M. Lewenstein, J. Martorell, A. Polls, Phys. Rev. A **81**, 023615 (2010).
 [13] J. I. Cirac, M. Lewenstein, K. Molmer, P. Zoller, Phys. Rev. A **57**, 1208 (1998).
 [14] M.J. Steel and M.J. Collett, Phys. Rev. **A57** 2920, (1998).
 [15] D. Dagnino, N. Barberán, M. Lewenstein, and J. Dalibard, Nature Phys. **5**, 431437 (2009).
 [16] P. Ziń, J. Chwedeńczuk, B. Oleś, K. Sacha and M. Trippenbach, Euro. Phys. Lett. **83** 64007 (2008).
 [17] "Quantum Theory of Tunneling" M. Razavy, World Scientific 2003.